Scripta Materialia 129 (2017) 35–38

Contents lists available at ScienceDirect

Scripta Materialia

journal homepage: www.elsevier.com/locate/scriptamat

Regular article

Effect of twin boundary segregation on damping properties in magnesium alloy

Hidetoshi Somekawa [a,*], Hiroyuki Watanabe [b], Dudekula Althaf Basha [a], Alok Singh [a], Tadanobu Inoue [a]

[a] Research Center for Structural Materials, National Institute for Materials Science, 1-2-1 Sengen, Tsukuba, Ibaraki 305-0047, Japan
[b] Osaka Municipal Technical Research Institute, 1-6-50 Morinomiya Joto-ku, 536-8553, Japan

ARTICLE INFO

Article history:
Received 6 September 2016
Received in revised form 14 October 2016
Accepted 15 October 2016
Available online xxxx

Keywords:
Magnesium alloy
Deformation twin
Damping capacity
Hardness
Segregation

ABSTRACT

The effect of solute segregation at deformation twin boundaries on the strength (hardness) and damping capacity was investigated using an extruded Mg-Y binary alloy. The existence of deformation twin brought about an increase in both the hardness and the damping capacity. However, a subsequent annealing had a different effect, in which segregation at twin boundaries led to a decrease in the damping capacity. This is because the segregation of yttrium stabilized the twin boundaries; as a result, these boundaries inhibited alternate shrinkage and growth of deformation twin, by which the vibration energy is absorbed.

Magnesium, which is the lightest among the structural metallic materials, is well-known to have a good damping capacity [1,2]. The structural components require development of metallic materials with high strength and high damping capacity. The addition of a solute element is one of the effective methods to increase the strength of the alloys. As for magnesium, many papers have reported the impact of alloying element on these properties [3–8]. Addition of a specific alloying element, e.g., nickel or copper, is sufficient to enhance damping capacity with maintaining a high strength. However, most alloying elements show a negative effectiveness; that is, many magnesium alloys have a lower damping capacity than that of pure magnesium [8]. This is due to the damping mechanism, i.e., a hysteresis-type basal dislocation damping. The solid solution alloying element plays a major role in the prevention of dislocation slip, leading to a high strength but low damping capacity. On the other hand, based on consideration of this damping mechanism, several papers have reported that the basal plane distribution, i.e., texture, is the controlling microstructural factor for the improvement of damping property [5,9,10]. Since the basal planes tend to align along the wrought processing direction, wrought-processed (e.g., rolled and extruded) magnesium and its alloys have a strong basal texture.

In addition to dislocation slip, deformation twin is also known to be another important mechanism during the plastic deformation of magnesium and its alloys at room temperature [11,12]. The $\{10\bar{1}2\}$-type deformation twin forms readily at the beginning of plastic deformation, and compensates for the lack of slip systems. This deformation twin has unique characteristics, i.e., twin growth and shrinkage against relationship between the crystal orientation and the applied stress direction. An alternate shrinkage and growth of deformation twin particularly plays a role in the absorption of vibration energy. Hence, recent papers have pointed out that this kind of twin is recognized as another essential microstructural feature for enhancing damping capacity [6,13–15]. Interestingly, a short-time annealing has been reported to bring about a further improvement of damping capacity due to a change in twin interface [14]. These twin-induced and annealed alloys also show good mechanical properties, e.g., high strength [16,17] and prevention for crack propagation [18], because of the segregation of the solute element at the twin boundaries. However, the impact of such difference in boundaries on the damping capacity remains unclear. In this study, yttrium was selected as the alloying element, because this element has a large atomic size difference with magnesium. The strength (hardness) and damping capacity were investigated using an extruded Mg-Y binary alloy, which had different microstructures, i.e., with and without (i) deformation twin existing in the matrix and (ii) segregation of the alloying element at the twin boundaries.

An extruded Mg-0.27 at.% (= 1.0 wt.%)Y binary alloy with a plate shape (thickness of 5 mm and width of 10 mm) was used in this study. The detailed chemical composition including impurities, material procedure, such as the extrusion condition, and initial microstructure were reported in our previous paper [19]. In brief, a cast alloy was extruded at the temperature of around 573 K. The extruded alloy was then annealed at a temperature of 573 K for 4 h (hereafter denoted as,

* Corresponding author.
E-mail address: SOMEKAWA.Hidetoshi@nims.go.jp (H. Somekawa).

http://dx.doi.org/10.1016/j.scriptamat.2016.10.019
1359-6462/

Table 1
Average basal {0002} <11$\bar{2}$0> Schmid factor, *S*, obtained by EBSD analysis and average Vickers hardness, *Hv*, after the various processed Mg-Y alloys.

	Material procedure	S	Hv
No twin-induced	As annealed	0.24	47.7
Without-HTed	As annealed -->compression	0.38	53.2
With-HTed	As annealed -->compression -->heat treatment	0.38	54.6

no twin-induced alloy). This no twin-induced alloy had an average grain size of 10 μm, and yttrium was segregated at the grain boundaries [19]. This no twin-induced alloy was compressed parallel to the extrusion direction at room temperature to induce the {10$\bar{1}$2}-type deformation twin into the matrix (hereafter denoted as, without-HTed alloy). The compressive strain and strain rate were 5 % and 1×10^{-3}/s, respectively. There are several reports that this compressive strain level of 5 % is the growth stage of the {10$\bar{1}$2}-type deformation twin [20,21]. The without-HTed alloy was annealed at the temperature of 423 K for 2.5 h (hereafter denoted as, with-HTed alloy) to stabilize the alloying element, i.e., yttrium, at the twin boundaries (twin boundary segregation). The denotation and material procedure of the above three alloys are listed in Table 1.

The microstructures of these two kinds of twin-induced alloys (without- and with-HTed alloys) were observed by the electron backscattered diffraction (EBSD, in a field emission gun scanning electron microscope (FE-SEM) equipped with an EDAX-TSL EBSD system) and transmission electron microscopy (TEM) equipped with a nano-sized beam for energy-dispersive X-ray spectroscopy (EDX). All of the microstructural observations were made in the middle of the plane containing the extrusion direction and the transverse direction. The samples for microstructural observation using EBSD method were prepared by polishing with fine SiC papers, diamond slurries and a colloidal alumina slurry. The polished samples were then chemically etched in a solution containing of HNO_3 (10 mL), acetic acid (30 mL), H_2O (40 mL) and ethanol (120 mL). The sample for TEM observation was prepared by grinding followed by thinning to perforation using an ion polishing system.

The strength and damping properties were investigated using three kinds of alloy samples (no twin-induced, without- and with-HTed alloys). The strength was evaluated by Vickers hardness measurements on a plane parallel to the extrusion direction in at least 10 locations. The damping capacity was examined by employing resonant frequency method in a cantilever holder at room temperature. The resonant frequency in the experimental apparatus was 13–15 Hz. The specimens for damping test had a rectangular shape with a length of 60 mm, a width of 10 mm and a thickness of 1.5 mm. The samples were prepared by machining in the direction parallel to the extrusion direction. The damping constant was specified by the loss factor, η, of free vibration, which is related to the logarithmic decrement, Λ, of $\eta = \Lambda/\pi$, in this study. The loss factor was measured at strain amplitudes ranging from ~5×10^{-5} to 5×10^{-4}.

The microstructures of the two twin-induced alloys are shown in Fig. 1 for (a) without-HTed alloy and (b) with-HTed alloy, respectively. Both the images are taken in the same region. These inverse pole figure maps show a number of lenticular shaped morphologies in the matrix, even after annealing at 423 K. According to EBSD analysis, these features are recognized as the {10$\bar{1}$2}-type deformation twin, which is well-known to form at the beginning of plastic deformation in magnesium and its alloys [11,20,22]. It is found that the microstructural feature of deformation twin does not show any change. The length fraction of the twin boundary, divided by the total boundary length including both grain and twin boundaries, is obtained to be 0.20 for both without-HTed and with-HTed alloys. The average grain size is measured to be approximately 10 μm, if we exclude the twin boundaries. The average grain sizes of the twin-induced alloys are the same as that of the no twin-induced alloy [19]. Basal plane pole figures obtained from EBSD analysis are inset in Fig. 1(a) and (b). Fig. 1(c) is the pole figure of no twin-induced alloy, which is obtained using the previous reported data [19]. Fig. 1(c) shows that the basal planes in most grains in the no twin-induced alloy align along the extrusion direction, indicating a basal texture, due to wrought processes. However, pole figure tendency in the two twin-induced alloys (Fig. 1(a) and (b)) are not the same as Fig. 1(c). Most of the grains tend to tilt to the transverse direction. This difference in texture distribution results from the formation of {10$\bar{1}$2}-type deformation twin. It is also noted that the peak intensities of the two twin-induced alloys are almost in similar ranges, and on the order of 3.7–4.0. Table 1 also includes the average Schmid factors of {0002}<11$\bar{2}$0> slip in each of the alloys obtained from EBSD analysis. The results of distribution in Schmid factor are not shown here; however, both of the two twin-induced alloys have the same distribution tendencies. The Schmid factor, which range between 0.4 and 0.5, is quite high fraction. Thus, the present annealing condition (423 K for 2.5 h) does not lead to occurrence of microstructural changes, such as grain growth, shrinkage/growth of twin boundaries and texture evolution.

A typical example of TEM observation of the with-HTed alloy is shown in Fig. 2. Fig. 2(a) shows a bright field image taken at a relatively low-magnification with diffraction pattern inset, and is confirmed to be a {10$\bar{1}$2}-type deformation twin, similar to that of EBSD observation. Fig. 2(b) is the high-angle annular dark-field (HAADF) image of the area enclosed with white dashed line in Fig. 2(a). The twin boundary is found to be sharp and show a bright contrast. EDX mapping around twin boundary, from the enclosed area, is inset on the top right in this

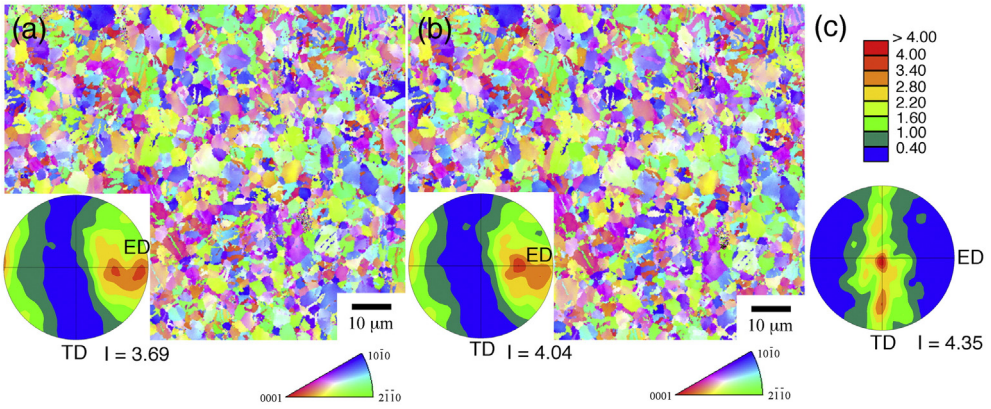

Fig. 1. The results of EBSD observations; (a) without-HTed, (b) with-HTed and (c) no twin-induced alloys. The corresponding pole figures of basal plane obtained from EBSD analysis are inset in each figure, and the pole figure image of no twin-induced alloy is from previously reported EBSD data [19]. ED and TD are the extrusion- and the transverse-directions, and *I* is the maximum peak intensity.